Band gap modulation of bilayer graphene by single and dual molecular doping: A van der Waals density-functional study

Tao Hu, I.C. Gerber

Chemical Physics Letters 616–617 (2014) 75–80

Contents lists available at ScienceDirect

Chemical Physics Letters

journal homepage: www.elsevier.com/locate/cplett

Editor's choice

Band gap modulation of bilayer graphene by single and dual molecular doping: A van der Waals density-functional study

Tao Hu[a,b], Iann C. Gerber[a,*]

[a] Université de Toulouse; INSA, UPS, CNRS; LPCNO 135 avenue de Rangueil, F-31077 Toulouse, France
[b] Department of Physics, Pukyong National University, Busan 608-737, South Korea

ARTICLE INFO

Article history:
Received 5 August 2014
In final form 15 October 2014
Available online 22 October 2014

ABSTRACT

Density functional calculations including long-range dispersion effects demonstrate that non-covalent doping with an electron donor acceptor couple of molecules can open an energy gap in a bilayer graphene. The band gap modulation can be controlled not only by the choice of adsorbed molecules (n-dopant versus p-dopant) but also by their concentration. A deep analysis of the charge transfer reveals that charge redistribution in bilayer graphene is the key issue for gap opening, due to the induced inversion symmetry breaking. The dual molecular non-covalent doping mode can achieve the opening of a gap up to 138 meV.

1. Introduction

Graphene has unique electronic transport [1,2], mechanical [3], and optical [4] properties that exhibit extraordinary potential for nanoelectronic applications [5–8]. However, pristine graphene, in the monolayer (MLG) or bilayer (BLG) states, is a gapless semimetal, thus limiting its applications in electronic nano-devices. Therefore, considerable efforts have been made to open band gaps in MLG or BLG. Both theoretical and experimental studies have demonstrated that a band gap can appear in the Bernal-stacking (AB-stacking) BLG, by breaking inversion symmetry [9–15], by applying an external electric field for instance [16–18], by breaking in-plane symmetry [19], by applying different homogeneous strains to the two layers [20] or by varying the interlayer spacing [21]. Molecular doping is also an alternative by provoking asymmetric charge distribution in graphene layers. In a non-covalent doping process of graphene, the carrier concentration, which is a key feature for electronics, can be controlled by the concentration of the adsorbed molecules, without introducing significant lattice deformation [22–25]. Currently, graphene growth process only allows molecular dopants to be absorbed on the topside of the graphene layers, although intercalation cannot be completely excluded. The bottom layer is usually doped by traditional substrates [26] or by specifically modified ones [27], see Refs. [28–30] for BLG cases.

Theoretically speaking, to yield accurate description of interlayer distances, to correctly describe the non-covalent interaction between graphene layers and charge transfer complexes in the density functional theory (DFT) framework it is mandatory to include nonlocal effects [31]. In previous theoretical reports on BLG doping, van der Waals forces are not explicitly taken into account [12,32], since traditional exchange-correlation functionals missed them. In this work we have used the so called van der Waals density functional (vdW-DF) [33–35], which has been successfully applied on layered [36,37] as well as on some molecular systems [38].

In this study, we report the doping of a Bernal-stacking BLG by several organic electron donor acceptor molecules as function of their adsorption modes. If one type of molecule (acceptor or donor) is adsorbed on a single side of the BLG, it corresponds to a single molecule doping mode. When at the same time, top and bottom layers are in interaction with a n-dopant and p-dopant, respectively, this hypothetical situation is called dual molecules doping mode throughout the article. Despite any experimental results on this specific setting have not been yet reported in the literature, one could imagine a three-steps procedure to realize it. By choosing first an appropriate molecule or atoms (donor or acceptor) that can easily intercalate between graphene layers or between a graphene layer and the substrate [39], and then by soft washing, some dopants should still remain bound on the downside of the BLG, due to larger binding energies. Finally, a dopant's solution with opposite character should be deposited, to transfer charge from/to the upper graphene layer. This setting also mimics in a sense the effect of an applied perpendicular electric field on the BLG by creating a dipole moment on an atomic length-scale. This directly relates to experimental works of Refs. [26,27].

* Corresponding author.
E-mail address: igerber@insa-toulouse.fr (I.C. Gerber).

http://dx.doi.org/10.1016/j.cplett.2014.10.034
0009-2614/

By using DFT calculations, we report that dual molecular doping can induce the opening of a significant band gap. It can be controlled as well as the carrier concentration, in a wider range by dual mode doping. As a consequence, a fine-tuning through the threshold voltage of the electronic conduction properties, that is a crucial issue for electronics application, is potentially achieved.

2. Method

We have studied a doped BLG system, in AB-stacking only, using periodic boundary condition within the supercell approach, with a vacuum region larger than 1.5 nm to avoid interaction between the periodic images. The calculations have been performed using the VASP code [40] with the Projected Augmented Wave (PAW) [41] pseudopotentials. The vdW-DF [42] functional is used for correlation and PBE for exchange [43]. An energy cutoff of 400 eV and care about k-point sampling have been taken to ensure energy convergence below few meV. The k-point grids are $3 \times 3 \times 1$ for large cells and $7 \times 7 \times 1$ for the smaller cells. The convergence criterion for calculations is that the force on each atom is smaller than 0.02 eV Å^{-1}. The Bader Charge Analysis method is used to estimate the charge transfer, using the program of G. Henkelman's group [44]. BLG is modeled either by a cell containing two (7×7) monolayers (98 carbon atoms each layer) or two (4×4) monolayers (32 carbon atoms each layer). It allows to discuss concentration's effects, with three possible concentrations: one molecule per 196 carbon atoms (0.51%) see Fig. 1, one molecule per 64 carbon atoms (1.56%) and one donor and one acceptor molecule per 196 carbon atoms (1%). These concentrations correspond to standard experimental settings of graphene molecular doping [45], and allow to avoid interaction between adsorbates within periodic boundary conditions. Three organic molecules, tetracyanoethylene (TCNE), tetrathiafulvalene (TTF), tetrakis(dimethylamino)ethylene (TDAE), are employed as dopant. As in Ref. [24], we have investigated all the possible adsorption sites on the BLG models, in terms of energetic and geometric aspects. They are very similar to the monolayer case, with very small energy differences between adsorption sites. Moreover the charge transfers from the different configurations are almost equal, as reported in a previous study [15]. Thus only structures, which minimize the total energy, are taken into consideration in the following.

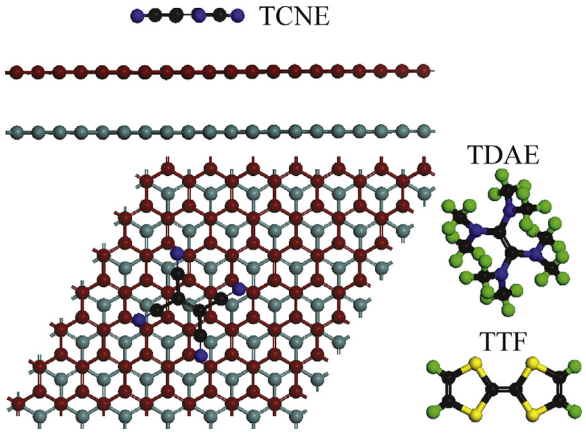

Fig. 1. Schematic view of three molecules adsorbed on a Bernal BLG. For an easier visualization, the carbon atoms of the two layers of BLG are in brown (upper layer) and cyan (bottom layer) respectively, while molecular carbon atoms are in black. Hydrogen atoms are in green, nitrogen in blue. (For interpretation of the references to color in this figure legend, the reader is referred to the web version of this article.)

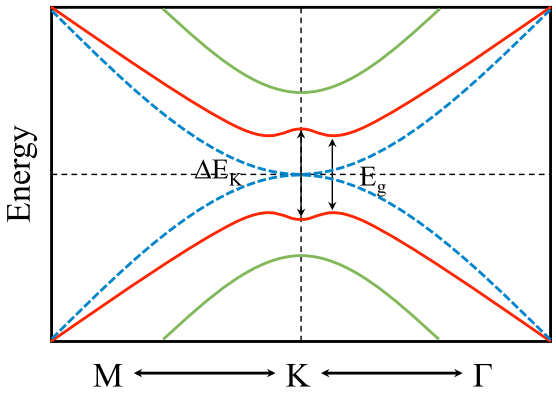

Fig. 2. Schematic band structure model of doped BLG close to the K point showing the "Mexican hat" dispersion (red lines). The dashed curves represent the quadratic dispersion of pristine BLG. The black dashed line corresponds to the Fermi level. (For interpretation of the references to color in this figure legend, the reader is referred to the web version of this article.)

3. Results and discussion

3.1. Electronic band structure of BLG

Accurate description of the band structure of pristine BLG is a prerequisite for a discussion of doped BLG electronic structures. In the Bernal stacking, pristine BLG band structure near the special K point of the reduced Brillouin zone, shows a quadratic dispersion, see Fig. 2. The π, π^* states and two lower energy bands are split in each valley by interlayer coupling [9,13], as in Fig. 3a which shows the DFT results. Two bands stand for the highest occupied π orbitals and the lowest unoccupied π orbitals (dashed blue). The corresponding electron and hole effective masses are calculated to be $0.045m_0$ and $0.056m_0$. These values agree very well with previous DFT estimates [15], but overestimate slightly experimental ones [46]: 0.041 and $0.036m_0$, respectively. The bands in green correspond to the two next levels. When the BLG is doped, a gap at the Dirac point K can appear (defined as ΔE_K) whereas the minimum separation between the bands is E_g. E_D can be defined as the energy difference between the middle of the band gap at K point and the Fermi level of the system. Thus, E_D, E_g and ΔE_K are equal to 0 for pristine BLG. Meanwhile, a doped BLG will possess the "Mexican hat" dispersion, the band gap (E_g) is no longer null. Moreover the energy level of the Dirac point can be shifted due to charge transfer.

3.2. Single molecular doping

3.2.1. Electron donor molecule doping

Band structures in Fig. 3c indicate that TTF's adsorption doesn't affect electronic structure of BLG except an upshift of Fermi level with an E_D value of 251 meV. This is in contradiction with the reported band gap of 80 meV [15]. One could first attribute this discrepancy to a concentration effect, since we have 1 TTF molecule per 98 C atoms, when 72 C atoms were used in Samuels' work. However when the concentration is increased, we only observe a larger shift of the Fermi level, without gap opening. So we may attribute this difference, to the different computational settings used and possibly to the exchange-correlation functional choice. The HOMO-derived state of the TTF molecule hybridizes with one of low-energy bands of the former Dirac crossing point. The charge transfer between the TTF molecule and the BLG is small 0.1 and 0.02 e depending on the concentration, as shown in Table 1.

One could expect that a stronger electron donor should be able to open a gap in a BLG. Since TDAE molecule has a low ionization energy that approaches those of alkali atoms [47,48] it should provide more electronic density to the carbon substrate than TTF

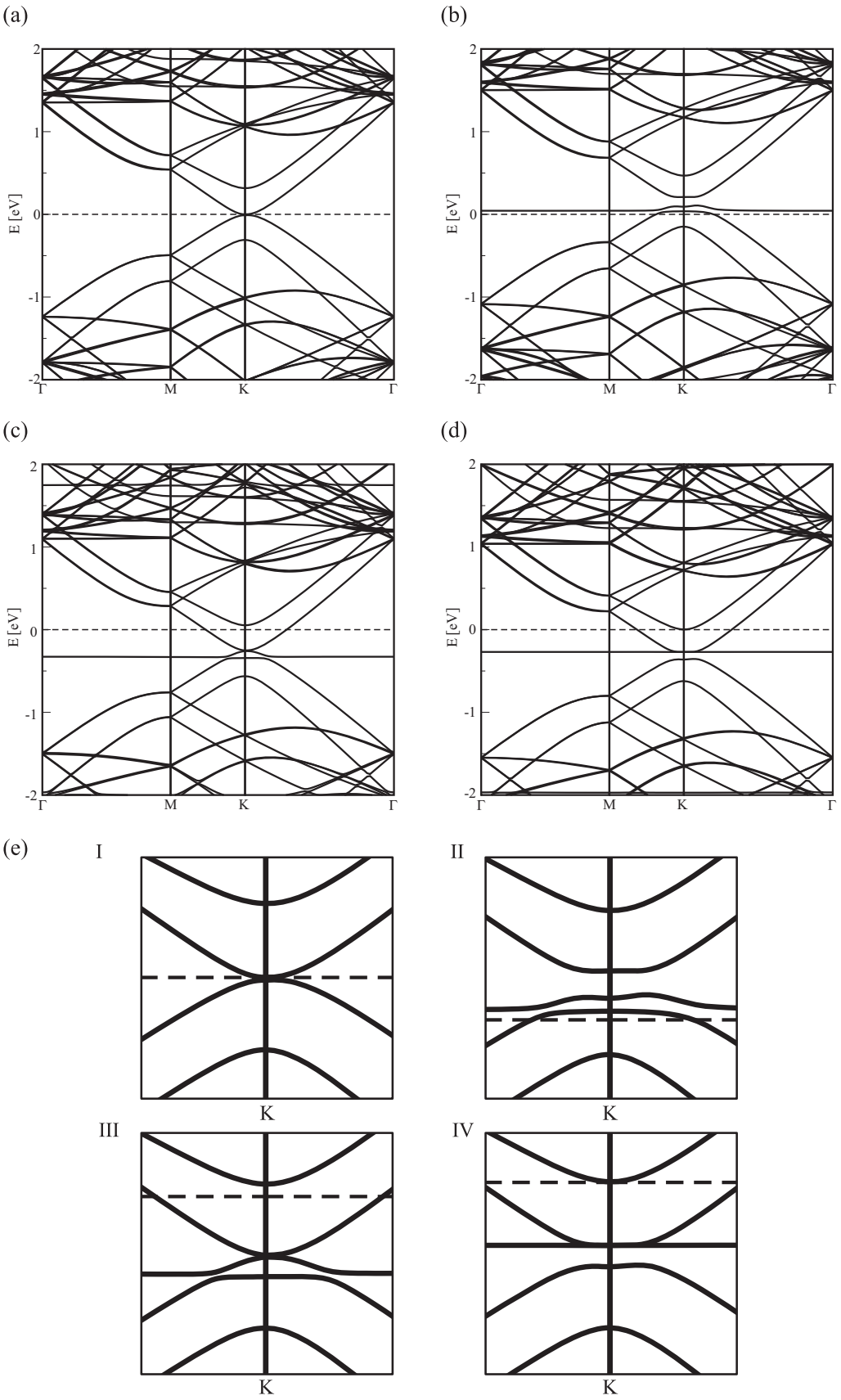

Fig. 3. Band structures of a pristine BLG and of doped BLGs with molecules adsorbed on one side only, calculated using vdW-DF functional, (a) Pristine BLG (7 × 7), (b) TCNE doped BLG (7 × 7), (c) TTF doped BLG (7 × 7), (d) TDAE doped BLG (7 × 7). (e) Four zoom-in figures (Around K point) corresponding to (a)–(d). The dashed line correspond to the Fermi level.

Table 1
Charge transfer (e) of molecules and each layer of BLG: a positive value means an increase of the electronic density when a negative one corresponds to a loss of the considered subsystem. Band gaps values (meV) and the Dirac point energy level shifts (meV) for each doped BLG systems are also included.

	0.51%			1.56%		
	TCNE	TTF	TDAE	TCNE	TTF	TDAE
CT Bottom layer	−0.18	0.03	0.13	−0.05	0.006	0.05
CT Top layer	−0.28	0.07	0.24	−0.23	0.011	0.12
CT Molecule	0.46	−0.1	−0.37	0.28	−0.017	−0.17
Band gap (E_g)	103	0	85	113	0	110
Dirac point energy level (E_D)	151	−251	−315	284	−413	−592

Table 2
Interlayer spacing (Å) of doped BLG and pristine BLG.

	TTF/BLG		TDAE/BLG		TCNE/BLG		BLG		Exp. [50]
	PBE	vdW	PBE	vdW	PBE	vdW	PBE	vdW	
Distance	4.16	3.43	4.15	3.43	4.11	3.60	3.98	3.41	3.35

does. Indeed, the TDAE molecule donates 0.37 e to the BLG. Clearly, the accumulations of charges in each layer are not identical (see Table 1). TDAE transfers 0.24 e to the top layer, and 0.13 e to the bottom layer, thus inducing carrier concentration of 9.3×10^{12} cm^{-2} and 5.1×10^{12} cm^{-2} on top and bottom layer respectively. These results show that the *n*-type doping by TDAE molecules is more efficient than by TTF ones. The electronic band structures are presented in Fig. 3d. A gap (85 meV) is opened in BLG when TDAE molecules are involved. The gap at the Dirac point K ($\mathbf{\Delta}E_K$) is 92 meV and the Dirac point energy level (E_D) is around 315 meV below the Fermi level. Adsorption of TDAE molecule provokes charge redistribution in graphene layer, which produces an electrostatic field perpendicular to graphene surface that breaks the symmetry of Bernal BLG. This leads to formation of a gap between $\boldsymbol{\pi}$ and $\boldsymbol{\pi}^*$ states. By increasing TDAE's concentration, charge transfer per carbon atom, defined as the total charge obtained by BLG divided by the total number of C atoms) is increased from 0.0019 to 0.0027 e. Consequently, the band gap is enlarged by 25 meV, E_D becomes −592 meV and $\mathbf{\Delta}E_K$ is around 124 meV. The doping effect is enhanced by a higher coverage of molecules.

3.2.2. Electron acceptor molecule doping

The adsorption of a TCNE molecule doesn't affect the atomic structure of the BLG. Moreover the total charge of the TCNE molecule is almost identical as with one molecule adsorbed on a MLG [24]. As for the donor molecule case, charge contributions of the two layers are asymmetric; the upper layer a little more charge (0.28 e) than the second one (0.18 e). This charge redistribution induced by TCNE's adsorption also causes a band gap opening as shown in Fig. 3b. The Dirac point energy level (E_D) lies 151 meV above the Fermi level, which suggests that the molecular has efficiently *p*-type doped the BLG. A band gap opening (E_g) of 103 meV is also found, when $\mathbf{\Delta}E_K$ is 117 meV. Our results are comparable with previous work [15], in which it is reported that F2-HCNQ obtains 0.51 e from BLG and opens a band gap of 118 meV. In the higher concentration case, TCNE receives less charges, while average charge contribution from BLG increases. The larger values of E_g, E_D, and $\mathbf{\Delta}E_K$, 113, 284 and 130 meV respectively, are a clear manifestation of a strong doping effect. The work function increases from 4.9 eV (low concentration) to 5.1 eV (high concentration), when the pristine value is 4.25 eV.

3.2.3. Effects of vdW dispersion corrections

Globally the charge transfer estimates when using standard PBE as exchange-correlation functional are very close to vdW-DF values but the BLG's electronic structure is very sensitive to the interlayer spacing [49]. Since PBE and vdW-DF provide different equilibrium distances between the two layers, see Table 2, the band structures of BLG calculated with PBE and vdW-DF functional are different. As expected the interlayer distance is overestimated with PBE functional, in comparison with experimental results, while the inclusion of nonlocal effects in the functional provides an acceptable separation despite of a little overestimation. For the TTF/BLG system, none of the two band structure calculations have a gap opening. But the Fermi level is more downshifted (by 50 meV) in PBE. When the TCNE molecule dopes the BLG, The doping is more significant for vdW-DF than for pure PBE calculations. The Dirac energy level (E_D) is around 151 meV above the Fermi level in both functionals. The corresponding E_g is 59 meV for PBE calculation, while the gap is larger when dispersion effects are taken into account. $\mathbf{\Delta}E_K$ are 87 and 117 meV, for PBE and vdW-DF estimates respectively. As already mentioned, different type of functionals provide

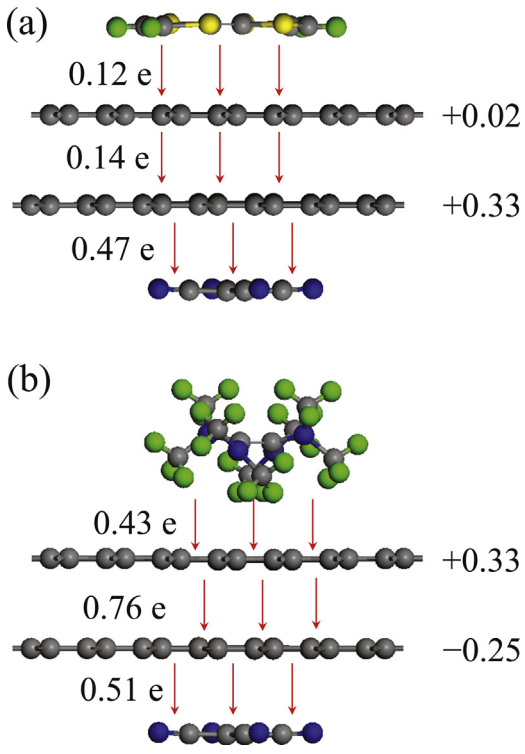

Fig. 4. (a) Side view of TTF/BLG/TCNE system and the corresponding charge transfers, (b) Side view of TDAE/BLG/TCNE system and the corresponding charge transfers. The values on the left are charge transfer from one subsystem to another, and values on the right are the charge possessed by corresponding layer.

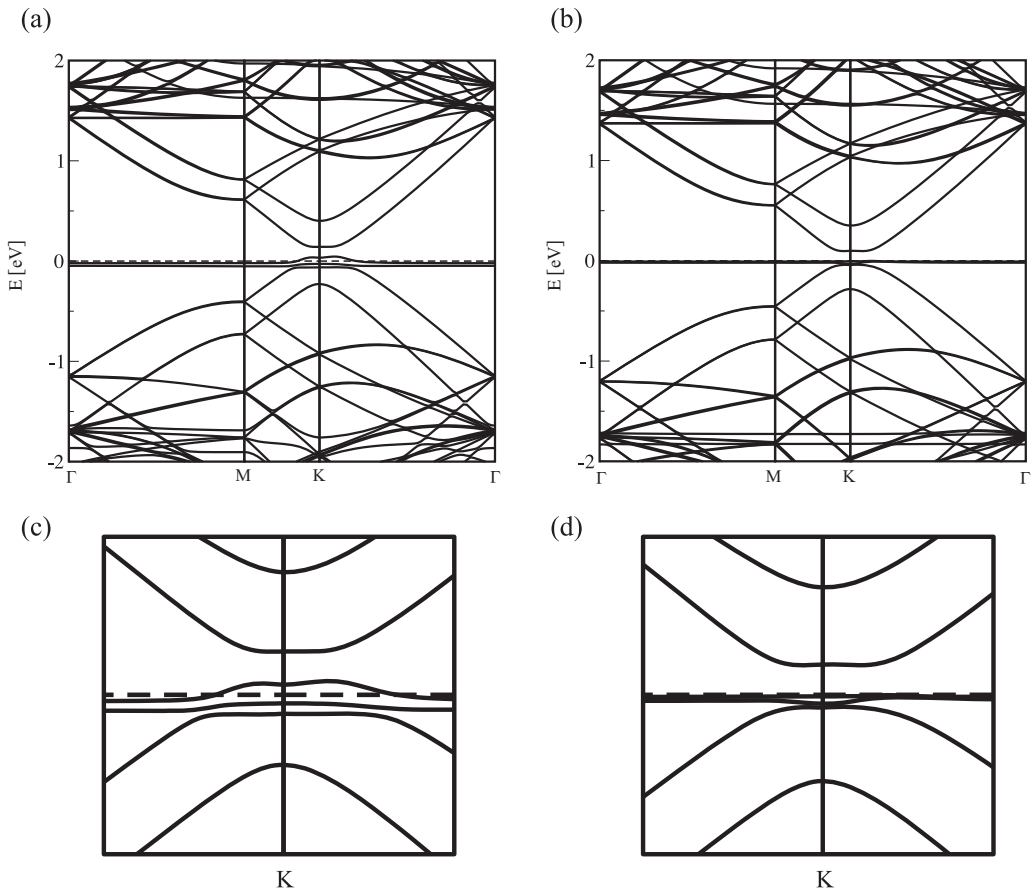

Fig. 5. Band structures for TTF/BLG/TCNE system (a) and TDAE/BLG/TCNE system (b). (c) and (d) are zoom-in figures around *K* point near the Fermi level for (a) and (b), respectively.

distinct equilibrium geometries which directly influence the electronic structure of the doped BLG.

3.3. Dual molecular doping

If one side molecular doping succeeds to open a band gap in a BLG it also shifts the Fermi level below or above the Dirac point depending on the type of molecules absorbed. Moreover the increase of the adsorbate's concentration enhances the doping, with larger shifts of the Fermi level, and larger band gaps values. Thus one could imagine to adjust band gap values with molecule's concentration. However, the increase of the band gap is limited due to a charge transfer saturation phenomenon already present at low concentration. The second major problem for potential applications is that the Fermi level is not lying in the band gap. In this respect, the dual molecules doping should help to counterbalance the Fermi level shift.

Two types of configurations have been addressed: one is with a TTF and a TCNE molecule adsorbed on the top and the bottom of the BLG. The second one uses TDAE and TCNE molecules as dopant. The corresponding side views of the optimized structures as well as the yielded charge transfers are presented in Fig. 4. In this dual doping mode, the TTF molecule provides a small amount of charge, while the TCNE molecule gets 0.47 e from the BLG, This electronic density mainly comes from the closest graphene layer but also from the TTF molecule. Indeed the upper layer is almost neutral, when the other one is positively charged. Since the TDAE molecule is a better donor than the TTF species, 0.43 e is thus transferred to BLG is the second case. At the same time the TCNE molecule receives 0.51 e. The upper layer, the one closer to the TDAE molecule, is now positively charged, whereas the second layer is now negatively charged. At the end, the BLG remains almost neutral, as of the charge has been entirely transferred from the TDAE to TCNE molecule, but polarizing the BLG.

Fig. 5 presents how dual doping mode affects the electronic band structures of the BLG. In the TTF/BLG/TCNE system, BLG is *p*-type doped ($E_D = 72$ meV) due to TCNE's stronger doping ability, with a band gap of 138 meV. This value is already larger than the one obtained in the single doping mode at the largest concentration. More importantly, the energy level of the Dirac point is now shifted back in the vicinity of the Fermi level. If a strong donor like TDAE is used then the Fermi level is now located at the maximum of the highest valence band, the BLG becomes a semi-conductor with a band gap of 100 meV. The electron and hole effective masses are drastically changed due to the gap opening, with values being $0.22m_0$ for the electron and $1.23m_0$ for the hole. This result proves that ideally one could image that a flexible band gap tuning can be realized by adjusting top and bottom molecule's concentration.

4. Conclusion

In summary, molecular doping provokes an asymmetry charge distribution in graphene layers, which in turn, causes a band gap opening in AB-stacking BLG. By increasing the concentration, doping is more efficient: larger shifts of the Fermi level and larger band gap values are obtained. Controlling molecule's concentration as well as the adsorption modes can modulate the BLG band gaps. We have shown that dual doping mode modulate the band gap value in a flexible way and tune the Dirac point energy levels (threshold voltage) easily. The obtained values of the band gap

using standard xc-functionals are certainly underestimated and more accurate values should be obtained either by using hybrid functionals or *GW* calculations, but this study like the one published in Ref. [15] provide first proofs of the concept of dual doping mode.

Acknowledgements

This work was supported by GENCI-CINES, GENCI-IDRIS through the project x2012096357 and project x2013096649. The authors would like to thank the CALcul en MIdi-Pyrénées (CALMIP, grant 2012/2013-P0812) for generous allocations of computer time. Finally, T. Hu would like to thank CSC-INSA program for financial support of his Ph.D. study

References

[1] K.S. Novoselov, Science 306 (2004) 666.
[2] A.H. Castro Neto, F. Guinea, N.M.R. Peres, K.S. Novoselov, A.K. Geim, Rev. Mod. Phys. 81 (2009) 109.
[3] C. Lee, X. Wei, J.W. Kysar, J. Hone, Science 321 (2008) 385.
[4] F. Wang, Y. Zhang, C. Tian, C. Girit, A. Zettl, M. Crommie, Y.R. Shen, Science 320 (2008) 206.
[5] Y.-M. Lin, A. Valdes-Garcia, et al., Science 332 (2011) 1294.
[6] M. Liu, et al., Nature 474 (2011) 64.
[7] Y. Zhang, et al., Nature 459 (2009) 820.
[8] F. Xia, T. Mueller, Y. Lin, A. Valdes-Garcia, P. Avouris, Nat. Nanotechnol. 4 (2009) 839.
[9] E. McCann, Phys. Rev. B: Condens. Matter 74 (2006) 161403.
[10] E. McCann, V.I. Fal'ko, Phys. Rev. Lett. 96 (2006) 086805.
[11] W. Zhang, et al., ACS Nano 5 (2011) 7517.
[12] X. Tian, J. Xu, X. Wang, J. Phys. Chem. B 114 (2010) 11377.
[13] T. Ohta, A. Bostwick, T. Seyller, K. Horn, E. Rotenberg, Science 313 (2006) 951.
[14] W.J. Yu, L. Liao, S.H. Chae, Y.H. Lee, X. Duan, Nano Lett. 11 (2011) 4759.
[15] A.J. Samuels, J.D. Carey, ACS Nano 7 (2013) 2790, 130227104203005.
[16] E.V. Castro, et al., Phys. Rev. Lett. 99 (2007) 216802.
[17] Z.Q. Li, et al., Phys. Rev. Lett. 102 (2009) 037403.
[18] S.B. Kumar, J. Guo, Appl. Phys. Lett. 98 (2011) 222101.
[19] X. Blase, A. Rubio, S.G. Louie, M.L. Cohen, Phys. Rev. B: Condens. Matter 51 (1995) 6868.
[20] S.-M. Choi, S.-H. Jhi, Y.-W. Son, Nano Lett. 10 (2010) 3486.
[21] Y. Guo, W. Guo, C. Chen, Appl. Phys. Lett. 92 (2008) 243101.
[22] Y.-H. Zhang, K.-G. Zhou, K.-F. Xie, J. Zeng, H.-L. Zhang, Y. Peng, Nanotechnology 21 (2010) 065201.
[23] Y.H. Lu, W. Chen, Y.P. Feng, P.M. He, J. Phys. Chem. B 113 (2009) 2.
[24] T. Hu, I.C. Gerber, J. Phys. Chem. C 117 (2013) 2411.
[25] L. Chen, L. Wang, Z. Shuai, D. Beljonne, J. Phys. Chem. Lett. 4 (2013) 2158.
[26] C. Coletti, et al., Phys. Rev. B: Condens. Matter 81 (2010) 235401.
[27] J. Park, et al., Adv. Mater. 24 (2012) 407.
[28] J.W. Yang, G. Lee, J.S. Kim, K.S. Kim, J. Phys. Chem. Lett. 2 (2011) 2577.
[29] T.H. Wang, Y.F. Zhu, Q. Jiang, J. Phys. Chem. C 117 (2013) 12873.
[30] T.H. Wang, Y.F. Zhu, Q. Jiang, Carbon 77 (2014) 431.
[31] J. Klimeš, D.R. Bowler, A. Michaelides, Phys. Rev. B: Condens. Matter 83 (2011) 195131.
[32] L. Liu, Z. Shen, Appl. Phys. Lett. 95 (2009) 252104.
[33] M. Dion, H. Rydberg, E. Schröder, D.C. Langreth, B.I. Lundqvist, Phys. Rev. Lett. 92 (2004) 246401.
[34] K. Berland, et al., J. Chem. Phys. 140 (2014) 18A539.
[35] P. Hyldgaard, K. Berland, E. Schröder, Phys. Rev. B: Condens. Matter 90 (2014) 075148.
[36] T. Björkman, A. Gulans, A.V. Krasheninnikov, R.M. Nieminen, J. Phys. Condens. Matter 24 (2012) 424218.
[37] T. Björkman, J. Chem. Phys. 141 (2014) 074708.
[38] A. Puzder, M. Dion, D.C. Langreth, J. Chem. Phys. 124 (2006) 164105.
[39] U. Starke, S. Forti, K.v. Emtsev, C. Coletti, MRS Bull. 37 (2012) 1177.
[40] G. Kresse, J. Hafner, Phys. Rev. B: Condens. Matter 47 (1993) 558.
[41] G. Kresse, D. Joubert, Phys. Rev. B: Condens. Matter 59 (1999) 1758.
[42] A. Gulans, M.J. Puska, R.M. Nieminen, Phys. Rev. B: Condens. Matter 79 (2009) 201105.
[43] J.P. Perdew, K. Burke, M. Ernzerhof, Phys. Rev. Lett. 77 (1996) 3865.
[44] W. Tang, E. Sanville, G. Henkelman, J. Phys. Condens. Matter 21 (2009) 084204.
[45] H. Kim, et al., Appl. Phys. Lett. 105 (2014) 011605.
[46] K. Zou, X. Hong, J. Zhu, Phys. Rev. B: Condens. Matter 84 (2011) 085408.
[47] M.R. Pederson, N. Laouini, J. Clust. Sci. 10 (1999) 557.
[48] H. Bock, H. Borrmann, Z. Havlas, H. Oberhammer, K. Ruppert, A. Simon, Angew. Chem. Int. Ed. Engl. 30 (1991) 1678.
[49] T. Ohta, A. Bostwick, J.L. McChesney, T. Seyller, K. Horn, E. Rotenberg, Phys. Rev. Lett. 98 (2007) 206802.
[50] G.E. Bacon, Acta Crystallogr. 4 (1951) 558.